Int J Clin Exp Med 2017;10(8):11606-11615
www.ijcem.com /ISSN:1940-5901/IJCEM0049731

Original Article

Value of IGFBPrP1 and contrast-enhanced ultrasound in liver fibrosis staging with rabbits

Haiyan Zhang[1,2,3*], Yun Zhang[4*], Xinghua Wang[5*], Xiaohong Guo[1,2,3], Huiqin Fan[2], Tingting Lv[1], Lixin Liu[1,2,3]

[1]Department of Gastroenterology and Hepatology, [2]Experimental Center of Science and Research, The First Hospital of Shanxi Medical University, Taiyuan, Shanxi Province, China; [3]Key Laboratory of Cell Physiology, Provincial Department of The Ministry of Education, Shanxi Medical University, Taiyuan, Shanxi Province, China; [4]Department of Infectious Disease, Heping Hospital, Changzhi Medical College, Changzhi, Shanxi Province, China; [5]Department of Ultrasound, The Second Hospital of Shanxi Medical University, Taiyuan, Shanxi Province, China. [*]Equal contributors.

Received September 21, 2016; Accepted April 25, 2017; Epub August 15, 2017; Published August 30, 2017

Abstract: Liver fibrosis is the outcome of a pathological process of repair in various liver injuries, and is important to diagnose efficiently and noninvasively. Although liver biopsy is regarded as the gold standard method to diagnose hepatic fibrosis, it is invasive and not easy to perform repeatedly. Our previous studies have shown that insulin-like growth factor binding protein-related protein 1 (IGFBPrP1) may be a novel molecule involved in the development of hepatic fibrogenesis. Contrast-enhanced ultrasound (CEUS) can assess microcirculation in the liver and is not associated with radiation hazards. Accordingly, this study aimed to explore the value of IGFBPrP1 and CEUS in liver fibrosis staging in a rabbit model. Healthy New Zealand rabbits were divided into a control group and experimental group, in which thioacetamide (TAA) administration was used to generate liver fibrosis. The histological characteristics of liver tissue were assessed using hematoxylin and eosin (HE) and Masson staining to stage from S0 to S4. Western blot revealed increases in liver tissue IGFBPrP1 levels in S0-S4 rabbits compared with the control group (P<0.05). Moreover, ELISA analysis revealed increased serum IGFBPrP1 levels in S0-S4 rabbits compared with control (P<0.05). Liver tissue and serum IGFBPrP1 levels demonstrated a significant positive correlation with liver fibrosis staging (P<0.05). After CEUS examination, relevant parameters were calculated, including hepatic artery arrival time (HAAT), portal vein arrival time (PVAT), hepatic vein arrival time (HVAT), hepatic artery to hepatic vein transit time (HAHVTT), portal vein to hepatic vein transit time (PVHVTT) and portal vein to hepatic artery transit time (HAPVTT). HAAT were shorter in S3-S4 rabbits than in the control group (P<0.05). Other parameters were shorter in S1-S4 rabbits than in the control group (P<0.05). Moreover, these parameters showed significant negative correlation with liver fibrosis staging (P<0.05). These results suggest that liver tissue and serum IGFBPrP1 levels, and CEUS parameters can reflect liver fibrosis stage and may be important contributors to the diagnosis of liver fibrosis and early-stage liver cirrhosis.

Keywords: IGFBPrP1, contrast-enhanced ultrasound, liver fibrosis, thioacetamide, rabbit

Introduction

Liver fibrosis is a common response to a variety of liver injuries and is characterized by excessive deposition of extracellular matrix (ECM). Recent studies have shown that liver fibrosis is a reversible step in the development of liver cirrhosis [1, 2]. Typically, patients with hepatic fibrosis exhibit no significant clinical signs, symptoms, or changes in the levels of serum biochemical markers. Therefore, liver fibrosis can advance to liver cirrhosis, and even hepatocellular carcinoma and liver failure [3-5]. Early identification and dynamic monitoring of liver fibrosis may significantly improve the prognosis of chronic liver diseases.

Currently, there are numerous methods available for diagnosing liver fibrosis including liver biopsy, serological testing, and radiological imaging [6]. Liver biopsy is regarded to be the gold standard; however, it is often avoided in clinical practice because of its invasiveness, sampling errors, and complications [7-9]. Although serological testing and radiological imaging are noninvasive, a definitive diagnosis is often not reached until late-stage liver cirrhosis. Thus, these particular tests lack accuracy in detect-

ing liver fibrosis and early-stage liver cirrhosis, and cannot be used to grade pathological changes [10-12]. Therefore, it would be advantageous to develop a simple, sensitive, highly specific, and noninvasive test for the identification of liver fibrosis and early-stage liver cirrhosis, and to evaluate pathological grade.

Our previous studies showed that insulin-like growth factor binding protein-related protein 1 (IGFBPrP1), also known as insulin-like growth factor binding protein 7 (IGFBP7), was significantly elevated in fibrotic and cirrhotic human liver specimens, and in mouse liver tissue with thioacetamide (TAA)-induced hepatic fibrosis [13, 14]. Moreover, we demonstrated that recombinant IGFBPrP1 was capable of triggering activation of hepatic stellate cells (HSCs) and ECM production both *in vitro* and *in vivo* [13, 15]. These findings suggest the potential of IGFBPrP1 to be a novel diagnostic marker of liver fibrosis.

In liver fibrosis, it is well-known that changes in hemodynamics, rather than significant morphological changes, are observed. With the development of contrast-enhanced ultrasound (CEUS) technology, an ultrasound (US) contrast reagent has been applied to evaluate organ perfusion. Examination of the microcirculation is limited with conventional US, Fibroscan, computed tomography (CT) and magnetic resonance imaging (MRI); however, it is possible using CEUS. CT is associated with radiation hazards and MRI is often too costly. Fibroscan lacks anatomical information and is influenced by various factors such as obesity and ascites [16-19].

TAA is a weak carcinogen that causes changes in hepatic fatty acid metabolism, which is consistent with the characteristics of human liver damage. Liver fibrosis and cirrhosis induced by TAA is a classical animal model that can provide valuable information in understanding pathological disease mechanisms [20, 21]. In the present study, we evaluated dynamic changes in IGFBPrP1 and a series of CEUS parameters, and attempted to validate their clinical value in diagnosing liver fibrosis and pathological grading in a rabbit model.

Materials and methods

Antibody and reagents

TAA was purchased from Sigma Aldrich (St. Louis, MO, USA). The protein extraction kit and protein quantification kit were from Applygen Technologies Incorporated (Beijing, China). The enhanced chemiluminescence (ECL) kit was from Thermo Scientific (Waltham, MA, USA). Antibodies against IGFBPrP1 and β-actin, and horseradish peroxidase (HRP)-labeled goat anti-mouse secondary antibody were from Santa Cruz Biotechnology (Santa Cruz, CA, USA). The IGFBPrP1 ELISA assay kit was from Shanghai Yifeng Biotechnology (Shanghai, China). The ultrasound contrast reagent (SonoVue) was obtained from Bracco Group (Milan, Italy).

Animal experiments

Healthy, 6-month-old male and female New Zealand rabbits, weighing between 2.0 kg and 3.0 kg (ID number: 2013 JIN 070001), were provided by the Taiyuan Institute of Animal Science (Taiyuan, China), and housed and fed in the animal care facility with a 12 h light-dark cycle at 22°C. All procedures were approved by the Taiyuan Institutional Animal Care and Use Committee. The rabbits were divided into the following groups: control (injected with saline [n=8]); experimental (injected subcutaneously with 4% TAA [1.0 mL/kg body weight, 2 times/week for 20 weeks [n=54]). Every two weeks, 2 to 4 rabbits were examined using CEUS. Liver tissues and sera were frozen at -80°C until further analysis. The effective dose of TAA was determined based on a mouse model of liver fibrosis and some preliminary studies. The optimal time point for euthanasia was chosen according to preliminary studies [14, 22].

Liver histology

Liver tissue was fixed in 10% neutral formalin. Next, paraffin-embedded liver tissue was cut into sections (5 μm thick) and stained with hematoxylin and eosin (HE) and Masson staining. The histological diagnosis of liver fibrosis was determined according to the Guidelines of Prevention and Treatment for Chronic Hepatitis B (2010 version) [23].

Western blot analysis

Proteins from frozen liver tissue were extracted according to the manufacturer's protocol. Tissue lysates were separated using sodium dodecyl sulfate-polyacrylamide gel electrophoresis and transferred to polyvinylidene fluoride membranes (Bio-Rad Laboratories, Hercules, CA, USA). The IGFBPrP1 protein was detected

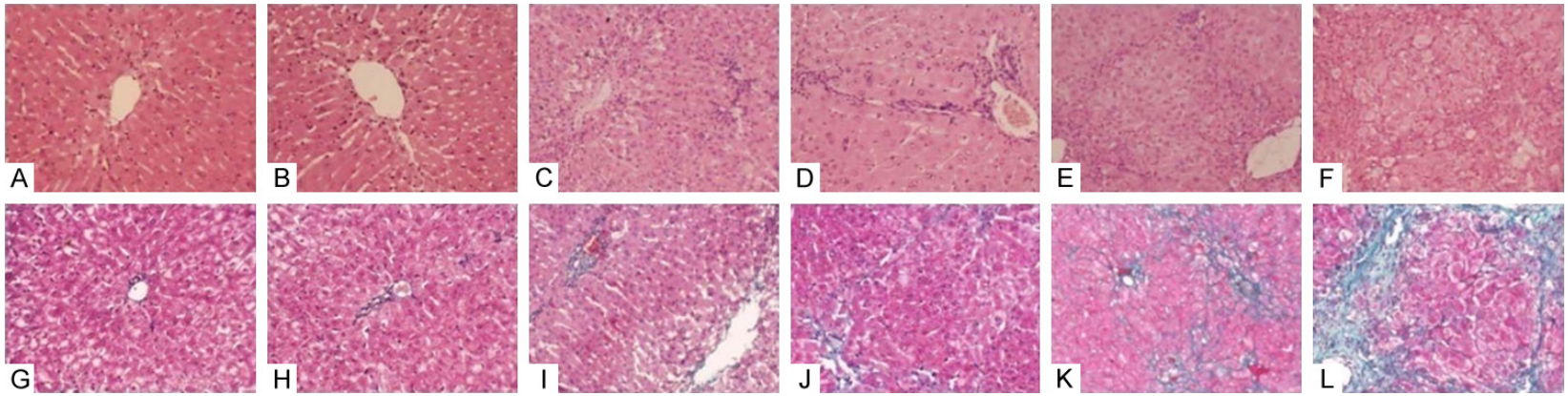

Figure 1. A-F. The histological characteristics of liver tissue in rabbits were assessed by HE staining, magnification ×200. A: Control group; B: S0 group; C: S1 group; D: S2 group; E: S3 group; F: S4 group. The pathological stage of liver tissue was determined using a 5-point scale: S0 (no fibrosis), S1 (portal area fibrosis or perisinusoid fibrosis), S2 (bridging fibrosis), S3 (numerous septal fibrosis without cirrhosis), S4 (early-stage cirrhosis). G-L. The formation of collagenous fiber in rabbit liver tissue were assessed by Masson staining, magnification ×200. G: Control group; H: S0 group; I: S1 group; J: S2 group; K: S3 group; L: S4 group.

Table 1. IGFBPrP1 levels of liver tissue in rabbits

Groups	n	IGFBPrP1/β-actin
Control	3	0.96±0.02
S0	3	1.04±0.02[a]
S1	3	1.08±0.01[a,b]
S2	3	1.09±0.01[a,b]
S3	3	1.11±0.02[a,b]
S4	3	1.12±0.03[a,b,c]
F		29.303
P		0.000

Note: [a]*P*<0.05 compared with control group; [b]*P*<0.05 compared with S0 group; [c]*P*<0.05 compared with S1 group.

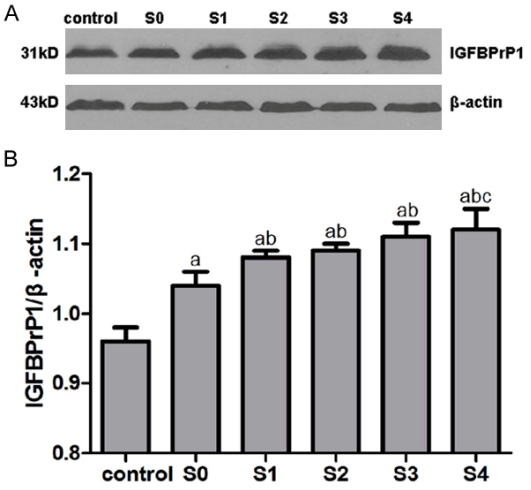

Figure 2. A. Protein expressions of IGFBPrP1 in rabbit liver tissue were examined by Western blot analysis. B. The relative protein levels were measured using Bio-Rad Quantity One software. [a]*P*<0.05 compared with control group; [b]*P*<0.05 compared with S0 group; [c]*P*<0.05 compared with S1 group.

Table 2. Serum IGFBPrP1 contents in rabbits

Groups	n	IGFBPrP1 (ng/ml)
Control	8	2.06±0.26
S0	7	5.18±0.33[a]
S1	14	5.60±0.67[a]
S2	6	5.61±0.53[a]
S3	7	8.26±1.01[a,b,c,d]
S4	5	8.39±0.88[a,b,c,d]
F		88.216
P		0.000

Note: [a]*P*<0.05 compared with control group; [b]*P*<0.05 compared with S0 group; [c]*P*<0.05 compared with S1 group; [d]*P*<0.05 compared with S2 group.

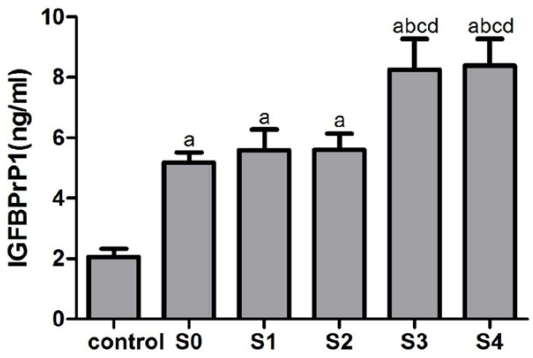

Figure 3. Serum IGFBPrP1 contents in rabbits were measured by ELISA analysis. [a]*P*<0.05 compared with control group; [b]*P*<0.05 compared with S0 group; [c]*P*<0.05 compared with S1 group; [d]*P*<0.05 compared with S2 group.

by immunoblotting with IGFBPrP1 antibody (1:500), β-actin antibody (1:1000), and HRP-conjugated secondary antibody (1:10000). Immunodetection was performed using a commercially available ECL detection system (ChemiDoc™ XRS Imaging System, Bio-RadLaboratories). The relative protein levels were measured using commercially available software (Quantity One, Bio-Rad Laboratories).

ELISA analysis

Blood samples were obtained and serum IGFBPrP1 was measured according to the ELISA kit instructions. Briefly, a standard sample was diluted to different concentrations to create a standard curve, and accordingly, serum levels of IGFBPrP1 were determined. All assays were performed in duplicate, and optical density at 450 nm was measured using an automatic microplate reader (Bio-Tek, Winooski, VT, USA).

CEUS

All ultrasonic examinations were performed by an experienced radiologist using a color ultrasonic diagnostic apparatus (Philips, Amsterdam, Netherlands) equipped with contrast pulse sequence technology; the mechanical index was set at 0.06 to 0.08. First, conventional two-dimensional US and color Doppler US were used to observe morphology, intrahepatic vessels of the liver, and the flow rate of the hepatic artery, portal vein, and hepatic vein. The mode was then switched to CEUS. SonoVue was rap-

Table 3. Parameters of CEUS (HAAT, PVAT and HVAT) in rabbits

Groups	n	HAAT (s)	PVAT (s)	HVAT (s)
Control	8	9.10±1.02	13.38±1.73	20.87±1.96
S0	7	8.75±1.63	12.63±1.11	20.00±1.81
S1	14	8.05±1.11	10.14±0.82[a,b]	16.29±1.65[a,b]
S2	6	7.61±0.88	9.45±0.84[a,b]	14.46±0.99[a,b,c]
S3	7	7.48±0.73[a]	9.05±0.75[a,b,c]	13.82±0.80[a,b,c]
S4	5	5.63±0.53[a,b,c,d,e]	6.82±0.44[a,b,c,d,e]	8.81±0.59[a,b,c,d,e]
F		7.626	34.576	54.153
P		0.000	0.000	0.000

Note: [a]*P*<0.05 compared with control group; [b]*P*<0.05 compared with S0 group; [c]*P*<0.05 compared with S1 group; [d]*P*<0.05 compared with S2 group; [e]*P*<0.05 compared with S3 group.

Table 4. Parameters of CEUS (HAHVTT, PVHVTT and HAPVTT) in rabbits

Groups	n	HAHVTT (s)	PVHVTT (s)	HAPVTT (s)
Control	8	11.78±2.13	7.49±2.32	4.29±1.01
S0	7	11.25±0.80	7.38±1.54	3.88±1.08
S1	14	8.25±0.95[a,b]	6.16±1.09[a]	2.09±0.81[a,b]
S2	6	6.85±0.59[a,b,c]	5.01±0.51[a,b]	1.84±0.50[a,b]
S3	7	6.34±0.97[a,b,c]	4.77±0.97[a,b,c]	1.56±0.72[a,b]
S4	5	3.18±0.65[a,b,c,d,e]	1.99±0.45[a,b,c,d,e]	1.19±0.32[a,b,c]
F		47.743	13.742	17.417
P		0.000	0.000	0.000

Note: [a]*P*<0.05 compared with control group; [b]*P*<0.05 compared with S0 group; [c]*P*<0.05 compared with S1 group; [d]*P*<0.05 compared with S2 group; [e]*P*<0.05 compared with S3 group.

idly infused through the cubital vein (0.1 mL/kg) followed by rapid infusion of 3 mL of saline. The following parameters were determined and restored by the QLAB-intensity curve software: hepatic artery arrival time (HAAT); portal vein arrival time (PVAT); hepatic vein arrival time (HVAT); hepatic artery to hepatic vein transit time (HAHVTT [HVAT - HAAT]); portal vein to hepatic vein transit time (PVHVTT [HVAT - PVAT]); and portal vein to hepatic artery transit time (HAPVTT [PVAT - HAAT]).

Statistical analysis

All data were analyzed using SPSS version 17.0 (SPSS, Inc., Chicago, IL, USA). The results were expressed as mean ± standard deviation (SD). One-way analysis of variance (ANOVA) with Dunnett's T3 post hoc test was used to compare values between different groups. Correlation analysis was performed using Spearman's correlation coefficient. *P*<0.05 was considered to be statistically significant.

Results

Pathological stage of liver tissue in rabbits

The histological characteristics of liver tissue from rabbits induced with TAA were examined using HE staining (**Figure 1A-F**) and Masson staining (**Figure 1G-L**), and diagnosed according to fibrosis stage as follows: S0 (n=7); S1 (n=14); S2 (n=6); S3 (n=7); and S4 (n=5). Fifteen rabbits died.

IGFBPrP1 levels of liver tissue in rabbits

Western blot analysis revealed that IGFBPrP1 levels in liver tissue were increased in S0-S4 rabbits compared with controls (*P*<0.05); increased in S1-S4 rabbits compared with S0 rabbits (*P*<0.05); and increased in S4 rabbits compared with S1 rabbits (*P*<0.05) (**Table 1** and **Figure 2A**, **2B**). Additionally, liver tissue IGFBPrP1 levels were positively and significantly correlated with liver fibrosis stage (r=0.914; *P*<0.05).

Serum IGFBPrP1 contents in rabbits

According to ELISA analysis, serum IGFBPrP1 contents were higher in S0-S4 rabbits than in the control group (*P*<0.05), and higher in S3-S4 rabbits than in the S0, S1 and S2 rabbits (*P*<0.05) (**Table 2** and **Figure 3**). Importantly, serum IGFBPrP1 levels were positively correlated with liver fibrosis stage (r=0.869; *P*<0.05).

Parameters of CEUS in rabbits

CEUS analysis revealed the following: PVAT, HVAT, HAHVTT, PVHVTT, and HAPVTT were shorter in S1 rabbits than controls (*P*<0.05), and PVAT, HVAT, HAHVTT, and HAPVTT were shorter than in S0 rabbits (*P*<0.05); PVAT, HVAT, HAHVTT, PVHVTT, and HAPVTT in S2 rabbits were shorter than in controls and S0 rabbits (*P*<0.05), and HVAT and HAHVTT were shorter than in S1 rabbits (*P*<0.05); HAAT, PVAT, HVAT, HAHVTT, PVHVTT, and HAPVTT were shorter in S3 rabbits than in controls (*P*<0.05), and PVAT, HVAT, HAHVTT, PVHVTT, and HAPVTT were shorter than in S0 rabbits (*P*<0.05), and PVAT, HVAT, HAHVTT, and PVHVTT were shorter than

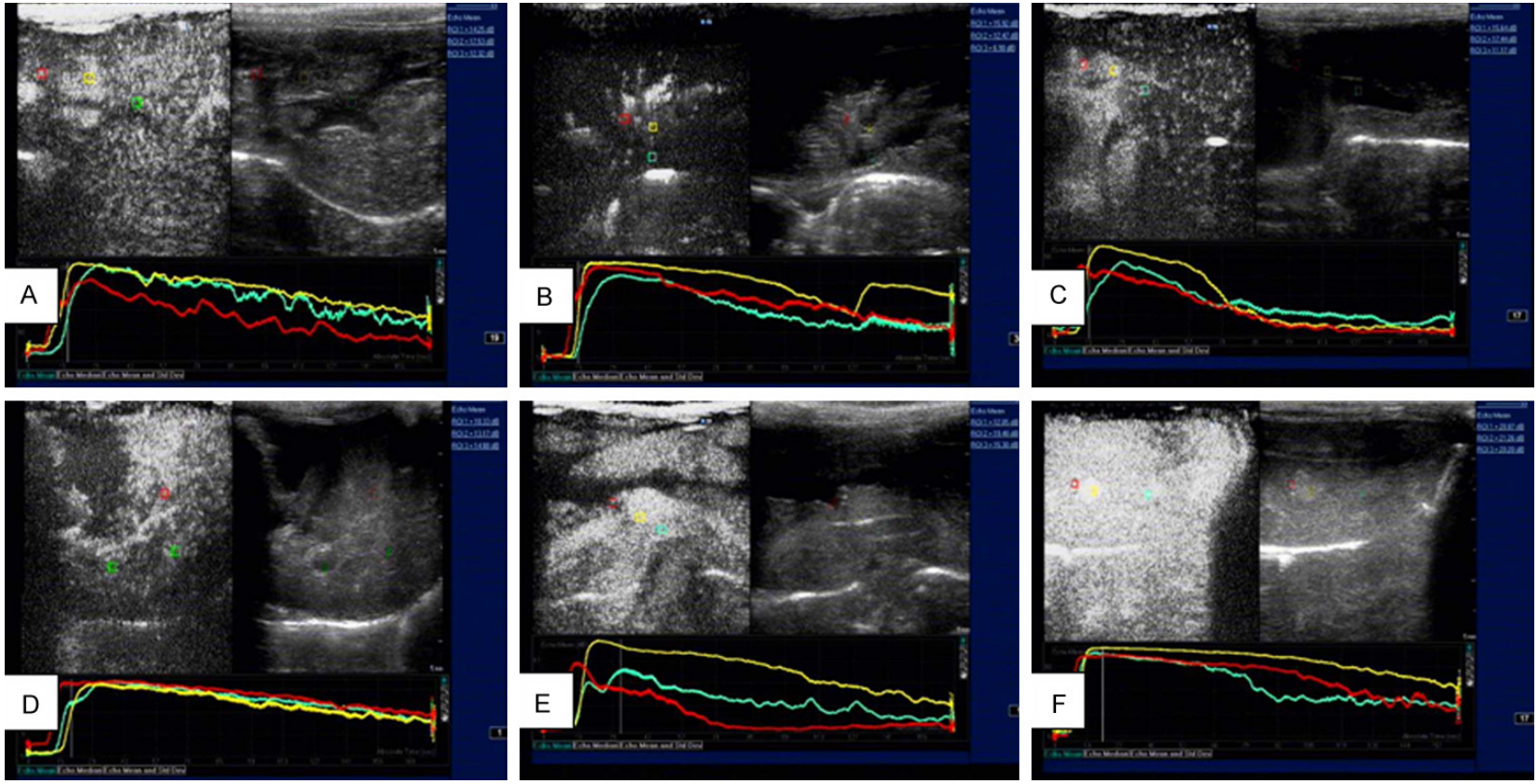

Figure 4. Time-intensity curve after infusion of ultrasound contrast of CEUS. Red: hepatic artery; yellow: portal vein; green: hepatic vein. A: Control group; B: S0 group; C: S1 group; D: S2 group; E: S3 group; F: S4 group.

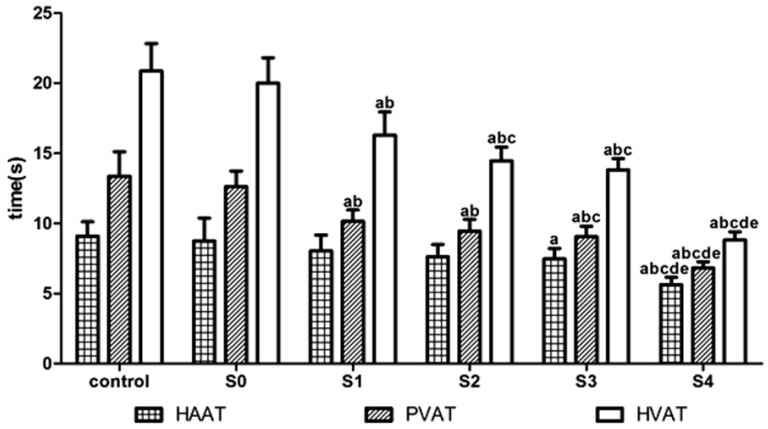

Figure 5. Parameters of CEUS were determined and restored by the QLAB-intensity curve software, including hepatic artery arrival time (HAAT), portal vein arrival time (PVAT) and hepatic vein arrival time (HVAT). [a]*P*<0.05 compared with control group; [b]*P*<0.05 compared with S0 group; [c]*P*<0.05 compared with S1 group; [d]*P*<0.05 compared with S2 group; [e]*P*<0.05 compared with S3 group.

in S1 rabbits (*P*<0.05); and finally, HAAT, PVAT, HVAT, HAHVTT, PVHVTT, and HAPVTT were shorter in S4 rabbits than in controls, and in S0 and S1 rabbits (*P*<0.05), and HAAT, PVAT, HVAT, HAHVTT, and PVHVTT were shorter than in S2 and S3 rabbits (*P*<0.05) (**Tables 3** and **4**; **Figures 4**-**6**). Moreover, HAAT, PVAT, HVAT, HAHVTT, PVHVTT, and HAPVTT demonstrated a significant negative correlation with liver pathological stage (r=-0.603, -0.870, -0.910, -0.895, -0.729 and -0.792, respectively; *P*<0.05).

Discussion

In the present study, TAA administration was used to generate a rabbit model of liver fibrosis. Liver fibrosis stages in rabbits were assessed using HE and Masson staining. In the normal group, liver cells were arranged regularly. Liver lobular architecture was intact, and few fibers formed in the blood vessel walls and biliary duct walls. In contrast, however, livers in the experimental group exhibited pathological characteristics in different stages such as portal area fibrosis or peri-sinusoid fibrosis, bridging fibrosis, numerous septal fibroses, and even the formation of pseudolobules.

IGFBPrP1 is a secreted protein and a member of the insulin-like growth factor family. It is extensively expressed in normal liver, kidney, breast, and skeletal muscles tissues, and body fluids such as blood and urine [24]. An increasing number of studies have shown that serum IGFBPrP1 may serve as a biomarker in some cancers including lung, breast and endometrial cancers [25-28]. Boers et al [29] found that expression of the IGFBPrP1 gene was significantly increased in the metaphase of HSC activation. Our previous studies demonstrated that IGFBPrP1 contributes to the development of liver fibrosis and may be involved in the progression of hepatic fibrogenesis. Our recent *in vitro* and *in vivo* studies revealed that IGFBPrP1 induces liver fibrosis by mediating the activation of HSCs via the Smad2/3 and ERK1/2 signaling pathway [30, 31]. In this study, liver tissue and serum levels of IGFBPrP1 in rabbits with TAA-induced fibrosis were increased compared with the control group (*P*<0.05). Furthermore, liver tissue and serum IGFBPrP1 levels demonstrated a significant and positive correlation with liver fibrosis stage (*P*<0.05). These findings suggest the promising potential of IGFBPrP1 as a novel diagnostic biomarker of liver fibrosis and early-stage liver cirrhosis.

Among radiological imaging methods, CEUS is not associated with radiation hazards and is less expensive than CT or MRI. Additionally, CEUS can assess microcirculation in the liver. Hepatic fibrosis is the outcome of a pathological process of repair in various liver injuries during which intrahepatic hemodynamics are altered. For example, activation of HSCs and sinusoid capillarization, leading to blood flow resistance, are increased. These changes result in a shunt between the portal and hepatic veins. In addition, ECM deposition and fiber separation can alter liver anatomy. Liver fibrosis may lead to reconstruction of hepatic lobules and formation of communicating branches between arteries and veins [32-34]. These factors caused changes in HAAT, PVAT, HVAT, HAHVTT, PVHVTT, and HAPVTT. They were shorter in the experimental group than in the-

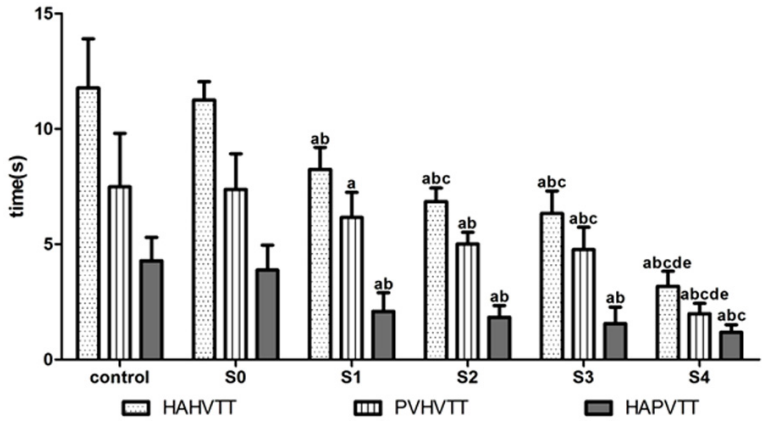

Figure 6. Parameters of CEUS also including hepatic artery to hepatic vein transit time (HAHVTT=HVAT-HAAT), portal vein to hepatic vein transit time (PVHVTT=HVAT-PVAT) and portal vein to hepatic artery transit time (HAPVTT=PVAT-HAAT). [a]*P*<0.05 compared with control group; [b]*P*<0.05 compared with S0 group; [c]*P*<0.05 compared with S1 group; [d]*P*<0.05 compared with S2 group; [e]*P*<0.05 compared with S3 group.

control group (*P*<0.05). Moreover, HAAT, PVAT, HVAT, HAHVTT, PVHVTT, and HAPVTT demonstrated a significant negative correlation with liver pathological stage (*P*<0.05). These results suggest that CEUS can mirror the changes in microcirculation and hemodynamics in liver fibrosis and early-stage liver cirrhosis.

Accurate diagnosis is often difficult using a single method, and all methods have inherent advantages and disadvantages. Examination of IGFBPrP1 combined with CEUS may improve the diagnostic efficiency of liver fibrosis and early-stage liver cirrhosis. Additional studies involving large animals (e.g., dogs) and humans are needed before our results can be appliedin clinical practice.

Conclusion

Dynamic observation of both IGFBPrP1 and CEUS in rabbits with TAA-induced liver fibrosis demonstrated that liver tissue and serum IGFBPrP1 levels and CEUS parameters can reflect liver fibrosis stage, and may be important contributors to the diagnosis of liver fibrosis and early-stage liver cirrhosis.

Acknowledgements

This study was funded by the National Natural Science Foundation of China (No.81141049 and No.81670559) and International Cooperation Foundation of Key Research and Development of Shanxi Province (No.201603-D421023).

Disclosure of conflict of interest

None.

Address correspondence to: Dr. Lixin Liu, Departments of Gastroenterology and Hepatology, The First Hospital of Shanxi Medical University, Mailbox 427, 85 Jiefang South Road, Taiyuan 030001, Shanxi Province, China. Tel: +86-351-4639075; Fax: +86-351-4639075; E-mail: lixinliu6@hotmail.com

References

[1] Tsochatzis EA, Bosch J and Burroughs AK. Liver cirrhosis. Lancet 2014; 383: 1749-1761.

[2] Wu Y, Liang Y, Zhu Y, Gao Y, Chen H, Zhang Y, Yin W, Li Y, Wang K and Xiao J. Protective effect of the omega-3 polyunsaturated fatty acids on the schistosomiasis liver fibrosis in mice. Int J Clin Exp Med 2015; 8: 9470-9476.

[3] Wallace MC and Friedman SL. Hepatic fibrosis and the microenvironment: fertile soil for hepatocellular carcinoma development. Gene Expr 2014; 16: 77-84.

[4] Sakurai T and Kudo M. Molecular link between liver fibrosis and hepatocellular carcinoma. Liver Cancer 2013; 2: 365-366.

[5] Kudo M. Advances in liver fibrosis imaging and hepatocellular carcinoma: update in 2013. Preface. Oncology 2013; 84 Suppl 1: 1-2.

[6] Bonnard P, Elsharkawy A, Zalata K, Delarocque-Astagneau E, Biard L, Le Fouler L, Hassan AB, Abdel-Hamid M, El-Daly M, Gamal ME, El Kassas M, Bedossa P, Carrat F, Fontanet A and Esmat G. Comparison of liver biopsy and noninvasive techniques for liver fibrosis assessment in patients infected with HCV-genotype 4 in Egypt. J Viral Hepat 2015; 22: 245-253.

[7] Asselah T, Marcellin P and Bedossa P. Improving performance of liver biopsy in fibrosis assessment. J Hepatol 2014; 61: 193-195.

[8] Awad Mel D, Shiha GE, Sallam FA, Mohamed A and El Tawab A. Evaluation of liver stiffness measurement by fibroscan as compared to liver biopsy for assessment of hepatic fibrosis in

children with chronic hepatitis C. J Egypt Soc Parasitol 2013; 43: 805-819.
[9] Madan K. Is liver biopsy still the gold standard for diagnosing liver fibrosis? Trop Gastroenterol 2011; 32: 253-255.
[10] Vergniol J, Boursier J, Coutzac C, Bertrais S, Foucher J, Angel C, Chermak F, Hubert IF, Merrouche W, Oberti F, de Ledinghen V and Cales P. Evolution of noninvasive tests of liver fibrosis is associated with prognosis in patients with chronic hepatitis C. Hepatology 2014; 60: 65-76.
[11] Coppola A, Di Capua M, Conca P, Cimino E, Tufano A, Cerbone AM, Di Minno G and Tarantino G. Noninvasive assessment of liver fibrosis in patients with chronic hepatitis C (and congenital bleeding disorders): where do we stand? Semin Thromb Hemost 2013; 39: 803-815.
[12] Alkhouri N and McCullough AJ. Noninvasive diagnosis of NASH and liver fibrosis within the spectrum of NAFLD. Gastroenterol Hepatol (N Y) 2012; 8: 661-668.
[13] Guo XH, Liu LX, Zhang HY, Zhang QQ, Li Y, Tian XX and Qiu ZH. Insulin-like growth factor binding protein-related protein 1 contributes to hepatic fibrogenesis. J Dig Dis 2014; 15: 202-210.
[14] Liu LX, Zhang HY, Zhang QQ and Guo XH. Effects of insulin-like growth factor binding protein-related protein 1 in mice with hepatic fibrosis induced by thioacetamide. Chin Med J (Engl) 2010; 123: 2521-2526.
[15] Liu LX, Huang S, Zhang QQ, Liu Y, Zhang DM, Guo XH and Han DW. Insulin-like growth factor binding protein-7 induces activation and transdifferentiation of hepatic stellate cells in vitro. World J Gastroenterol 2009; 15: 3246-3253.
[16] Zhao H, Chen J, Meixner DD, Xie H, Shamdasani V, Zhou S, Robert JL, Urban MW, Sanchez W, Callstrom MR, Ehman RL, Greenleaf JF and Chen S. Noninvasive assessment of liver fibrosis usingultrasound-based shear wave measurement and comparison to magnetic resonance elastography. J Ultrasound Med 2014; 33: 1597-1604.
[17] Liu GJ, Ji Q, Moriyasu F, Xie XY, Wang W, Wong LH, Lin MX and Lu MD. Value of contrast-enhanced ultrasound using perflubutane microbubbles for diagnosing liver fibrosis and cirrhosis in rats. Ultrasound Med Biol 2013; 39: 2158-2165.
[18] Ying M, Leung G, Lau TY, Tipoe GL, Lee ES, Yuen QW, Huang YP and Zheng YP. Evaluation of liver fibrosis by investigation of hepatic parenchymal perfusion using contrast-enhanced ultrasound: an animal study. J Clin Ultrasound 2012; 40: 462-470.
[19] Orlacchio A, Bolacchi F, Petrella MC, Pastorelli D, Bazzocchi G, Angelico M and Simonetti G. Liver contrast enhanced ultrasound perfusion imaging in the evaluation of chronic hepatitis C fibrosis: preliminary results. Ultrasound Med Biol 2011; 37: 1-6.
[20] Wallace MC, Hamesch K, Lunova M, Kim Y, Weiskirchen R, Strnad P and Friedman SL. Standard operating procedures in experimental liver research: thioacetamide model in mice and rats. Lab Anim 2015; 49: 21-29.
[21] Tennakoon AH, Izawa T, Wijesundera KK, Katou-Ichikawa C, Tanaka M, Golbar HM, Kuwamura M and Yamate J. Analysis of glial fibrillary acidic protein (GFAP)-expressing ductular cells in a rat liver cirrhosis model induced by repeated injections of thioacetamide (TAA). Exp Mol Pathol 2015; 98: 476-485.
[22] Xu JJ, Liu LX, Zhang QQ and Zhang HY. [The protective effect and mechanism of anti-IGFBPrP1 antibody for hepatic fibrosis induced thioacetamide]. Zhonghua Gan Zang Bing Za Zhi 2009; 17: 464-465.
[23] [The guideline of prevention and treatment for chronic hepatitis B (2010 version)]. Zhonghua Gan Zang Bing Za Zhi 2011; 19: 13-24.
[24] Oh Y, Nagalla SR, Yamanaka Y, Kim HS, Wilson E and Rosenfeld RG. Synthesis and characterization of insulin-like growth factor-binding protein (IGFBP)-7. Recombinant human mac25 protein specifically binds IGF-I and -II. J Biol Chem 1996; 271: 30322-30325.
[25] Smith E, Ruszkiewicz AR, Jamieson GG and Drew PA. IGFBP7 is associated with poor prognosis in oesophageal adenocarcinoma and is regulated by promoter DNA methylation. Br J Cancer 2014; 110: 775-782.
[26] Rupp C, Scherzer M, Rudisch A, Unger C, Haslinger C, Schweifer N, Artaker M, Nivarthi H, Moriggl R, Hengstschlager M, Kerjaschki D, Sommergruber W, Dolznig H and Garin-Chesa P. IGFBP7, a novel tumor stroma marker, with growth-promoting effects in colon cancer through a paracrine tumor-stroma interaction. Oncogene 2015; 34: 815-825.
[27] Meersch M, Schmidt C, Van Aken H, Martens S, Rossaint J, Singbartl K, Gorlich D, Kellum JA and Zarbock A. Urinary TIMP-2 and IGFBP7 as early biomarkers of acute kidney injury and renal recovery following cardiac surgery. PLoS One 2014; 9: e93460.
[28] Liu L, Yang Z, Zhang W, Yan B, Gu Q, Jiao J and Yue X. Decreased expression of IGFBP7 was a poor prognosis predictor for gastric cancer patients. Tumour Biol 2014; 35: 8875-8881.
[29] Boers W, Aarrass S, Linthorst C, Pinzani M, Elferink RO and Bosma P. Transcriptional profiling reveals novel markers of liver fibrogenesis:

gremlin and insulin-like growth factor-binding proteins. J Biol Chem 2006; 281: 16289-16295.

[30] Zhang Y, Zhang QQ, Guo XH, Zhang HY and Liu LX. IGFBPrP1 induces liver fibrosis by inducing hepatic stellate cell activation and hepatocyte apoptosis via Smad2/3 signaling. World J Gastroenterol 2014; 20: 6523-6533.

[31] Guo Y, Zhang Y, Zhang Q, Guo X, Zhang H, Zheng G and Liu L. Insulin-like growth factor binding protein-related protein 1 (IGFBPrP1) contributes to liver inflammation and fibrosis via activation of the ERK1/2 pathway. Hepatol Int 2015; 9: 130-141.

[32] Ridolfi F, Abbattista T, Busilacchi P and Brunelli E. Contrast-enhanced ultrasound evaluation of hepatic microvascular changes in liver diseases. World J Gastroenterol 2012; 18: 5225-5230.

[33] Ridolfi F, Abbattista T, Marini F, Vedovelli A, Quagliarini P, Busilacchi P and Brunelli E. Contrast-enhanced ultrasound to evaluate the severity of chronic hepatitis C. Dig Liver Dis 2007; 39: 929-935.

[34] Sugimoto K, Shiraishi J, Moriyasu F, Ichimura S, Metoki R and Doi K. Analysis of intrahepatic vascular morphological changes of chronic liver disease for assessment of liver fibrosis stages by micro-flow imaging with contrast-enhanced ultrasound: preliminary experience. Eur Radiol 2010; 20: 2749-2757.